

Supplementary Information

Precipitation-based Colorimetric Multiplex Immunoassay in Hydrogel Particles

Yoon Ho Roh^{a,‡}, Hyun Jee Lee^{a,‡}, Ju Yeon Kim^a, Hyeon Ung Kim^a, Sun Min Kim^{b,*}, and Ki Wan Bong^{a,*}

^a Department of Chemical and Biological Engineering, Korea University, Seoul 02841, Republic of Korea

^b Department of Obstetrics and Gynecology, Seoul Metropolitan Government-Seoul National University Boramae Medical Center, Seoul 07061, Republic of Korea

*Correspondence addressed to: bong98@korea.ac.kr, obgysun@gmail.com

‡These authors contributed equally.

Design of encoded hydrogel microparticles

Hydrogel microparticles are lithographically encoded by designing circular photomasks with or without 8 rectangles combined (Fig.S1). From this design, 35 possible codes could be easily created. Furthermore, we can expand the code numbers more than hundreds by adding and combining shapes located at the end of the circle as semi-circles or triangles as well as rectangles. The height of the particles was optimized in order to take x-y plane images of hydrogel particles after the reaction. Note that the aspect ratio, defined as height/width, is ~ 0.23 .

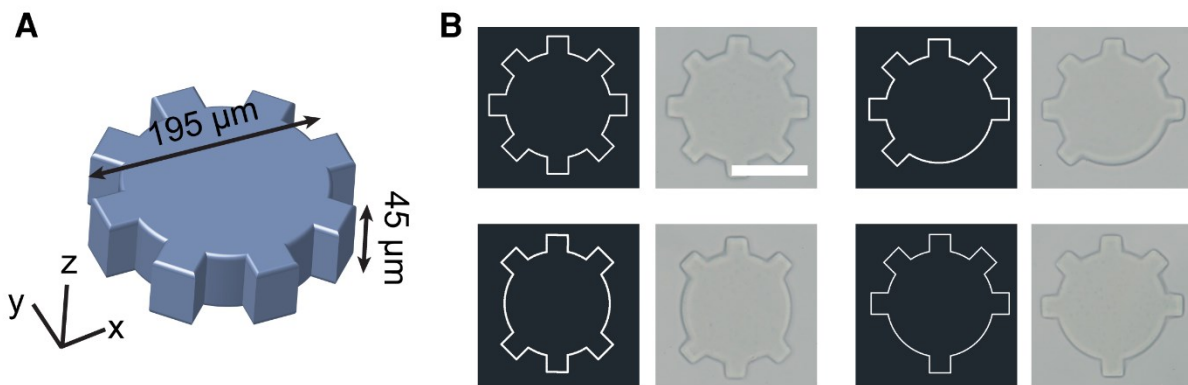


Figure S1. Design of encoded hydrogel microparticles. a) Geometry of encoded hydrogel microparticles. b) Expansion of code numbers in hydrogel microparticles. Images with black background are photomask patterns designed by AutoCAD and images with gray background are micrograph of synthesized particles by each photomask (scale bar, 100 μm).

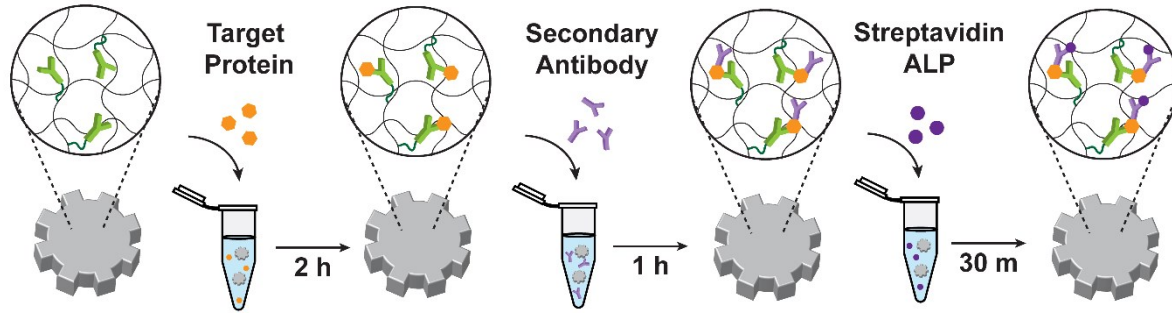


Figure S2. Schematic view of the immunoassay. Antibody functionalized hydrogel microparticles are mixed with target proteins and after the reaction, secondary antibodies are added to label biotin at target binding site. Then, streptavidin-ALP is added for the further enzyme-substrate interaction.

Characterization of colorimetric reaction

Insoluble coloured products are synthesized by enzyme-substrate interaction. In this reaction, alkaline phosphatase (ALP) hydrolyzes BCIP (5-bromo-4-chloro-3-indolyl phosphate) into intermediate which dimerizes to form an insoluble indigo dye and two hydrogen atoms resulting from BCIP dimerization reduce nitro blue tetrazolium (NBT) to insoluble diformazan. Insoluble products are aggregated inside the hydrogel networks due to the surrounding hydrophilic condition. As the colour development process is based on enzyme-substrate interaction, we used Michaelis-Menten equation to explain the kinetics of colorimetric reaction.

$$\frac{d[P]}{dt} = \frac{k_3[S][E]_0}{K_M + [S]} \quad (1)$$

Where $[P]$ is the concentration of the product, k_3 is the catalytic rate constant, $[S]$ is the substrate concentration, $[E]_0$ is the initial enzyme concentration and K_M is the Michaelis-Menten constant. In our case, $[S]$ is in great excess than K_M ¹ and therefore, we obtain

$$\frac{d[P]}{dt} = k_3[E]_0 \quad (2)$$

Integrating Eq. (2) gives

$$P = ak_3[E]_0t \quad (3)$$

where P is the colorimetric intensity of the product and a is the signal efficiency factor that takes into account detector efficiency. By performing colorimetric reaction after the immunoassay procedures with PIGF at the concentration of 2048 pg mL^{-1} , we found that the colorimetric intensities were increased linearly according to the time as expected from the Michaelis-Menten equation. This results indicate that the colorimetric intensities are dependent of time and initial enzyme concentration. To verify this relationship, we calculated the signal efficiency factor and applied to the different concentrations of PIGF. In order to obtain the signal efficiency factor, initial enzyme concentration $[E]_0$ was first calculated by utilizing streptavidin-r-phycoerythrin (SAPE) instead of streptavidin-ALP. We measured the fluorescent intensity of SAPE solution in the microfluidic channel where the height of channel is equal to the height of the particle. By evaluating various concentrations of SAPE solution, we created a standard calibration curve which can convert measured fluorescent intensity to known SAPE concentration (Fig. S3). Then, we measured the fluorescent intensity of particles reacted with PIGF at the concentration of 2048 pg mL^{-1} and translated into the concentration of SAPE, which is $4.9 \times 10^{-5} \text{ mM}$ per single particle. Note that the concentration of SAPE was assumed to be equal to the concentration of streptavidin-ALP. This assumption is reasonable because both of streptavidin conjugates are in large excess than the biotin and the size of SA-ALP and SAPE ($\sim 146 \text{ kDa}$ and $\sim 300 \text{ kDa}$, respectively) are within a diffusible range towards the hydrogel networks². By utilizing rate constant³ of $k_3 \sim 30 \text{ s}^{-1}$ and the slope value obtained from the experiment (ratio of the change in the colorimetric intensities of particles reacted

with PIGF at the concentration of 2048 pg mL⁻¹ over the change in the time), signal efficiency factor was calculated as 35.17 AU mM⁻¹.

Then, we adapted Eq. (3) to various concentrations of PIGF. The initial enzyme concentration in particle for each PIGF concentration (512, 1024, 7500 pg mL⁻¹) was calculated by exploiting a standard calibration curve. The experimental results of the colorimetric intensities according to the various PIGF concentrations were nicely fitted to the estimated line (Fig. 2a). The model's goodness of fit was analyzed based on the sum of normalized mean squared errors subtracted from 1. The fit values for 7500, 2048, 1024, 512 pg/mL cases were 0.989, 0.991, 0.887, 0.934, respectively.

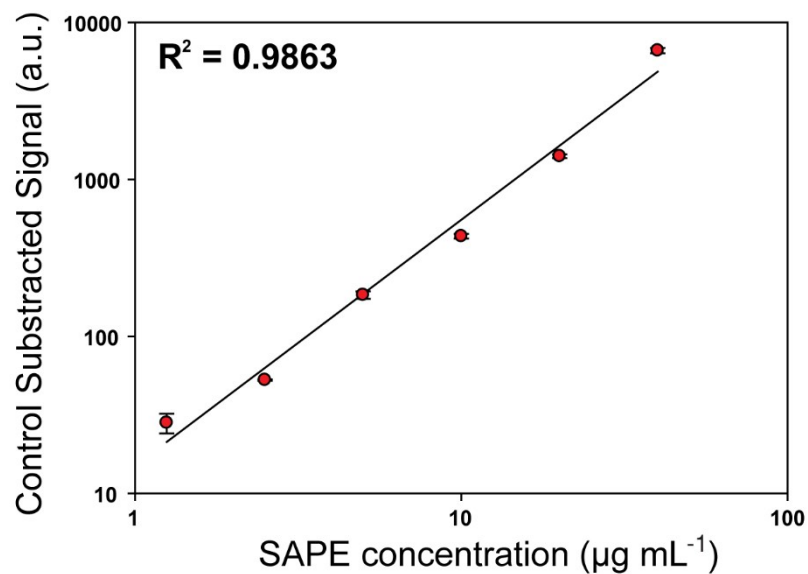


Figure S3. Standard calibration curve for SAPE solution inside the microchannel. Each data point and the vertical error bars represent the average signal and standard deviation of 7 particles.

Estimation of Damköhler number

Damköhler number can be defined by following equation,

$$Da = \frac{k_a P_0 L^2}{D_{gel}}$$

where k_a is the forward rate constant, P_0 is the concentration of incorporated probe, L is the distance from the center of the particle to edge, and D_{gel} is the diffusivity of the target in the hydrogel matrix. To calculate Da values, we used parameters D_{gel} of 5.66×10^{-11} m²/s and k_a of 10^5 M⁻¹ s⁻¹ that had been previously obtained based on the 150 kDa fluorescently labeled antibody, which has similar molecular weight with sEng^{4,5}. For P_0 , we used 8.2×10^{-4} mol m⁻³, considering that the PSF method provides 8.2 times enhanced probe loading density⁶ and for L , we used 75 μm. Calculated sEng specific Da value is ~8 which represents limited diffusion of our system.

In order to characterize the specific Da values of other proteins including PIGF (34 kDa) and sFlt-1 (90 kDa), we need to experimentally measure their diffusivity and association constant. However, we can roughly estimate that the other proteins have same order of Da value as same as sEng since diffusivity and association constant only vary up to ~2.5 times in this molecular weight range^{7,8}. Estimated Damköhler number is within an optimal range for high performance of HCI since the probe concentration and diffusivity had been previously optimized for the assay.

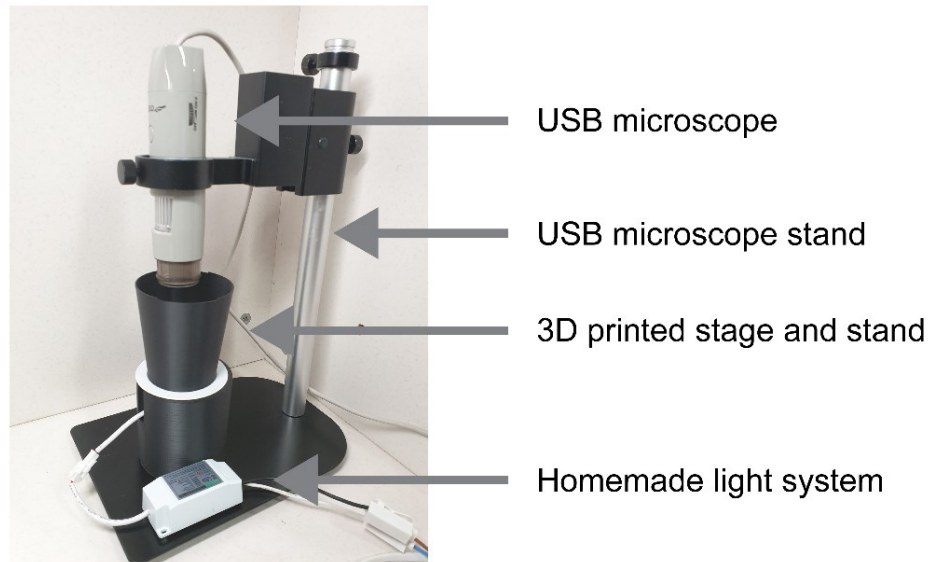


Figure S4. Instrument for obtaining bright field micrographs of encoded hydrogel microparticles. The instrument is mainly divided into two parts: USB microscope fixed by microscope stand and 3D printed stand combined with homemade light system. USB microscope take images of microfluidic channel on the top of the 3D printed stand with the aid of light from the below. We installed a diffuser plane on a light source in order to get an image with uniform background.

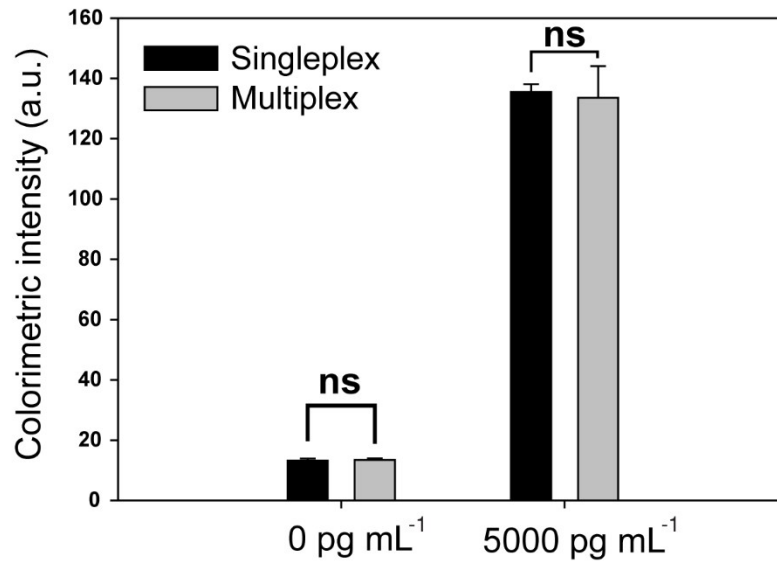


Figure S5. Investigation of interference during the colorimetric reaction. Encoded hydrogel microparticles after the immunoassay with 0 pg mL⁻¹ and 5000 pg mL⁻¹ of PIGF reactions were carried out by combining or separating the particles of each group (reacted with 0 pg mL⁻¹ or 5000 pg mL⁻¹) in order to identify the interference of synthesized coloured products. No statistical differences were found according to the combining or separating the particles during the colorimetric reaction, representing that the synthesized coloured products form a particle does not interfere with colorimetric intensity of other particles (n=7). Statistical significance was evaluated using Mann-Whitney U test.

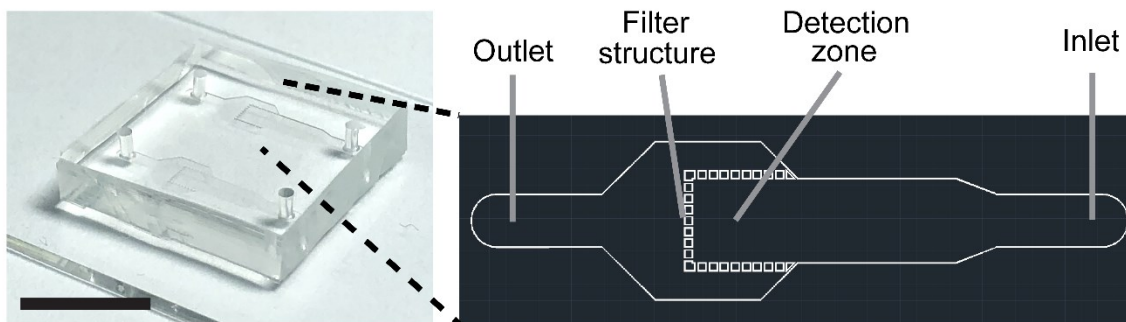


Figure S6. Design of microfluidic channel for particle collection and imaging. Bright field image of PDMS microfluidic chip (left) and photomask patterns designed by AutoCAD (right). Microfluidic channel consists of inlet, detection zone, filter structure and outlet. Inserted microparticles from inlet collected at the detection zone by filter structure which are arranged at intervals of 5 μm . Excessive buffer injected more than the volume of channel flows out through the outlet (scale bar, 1cm).

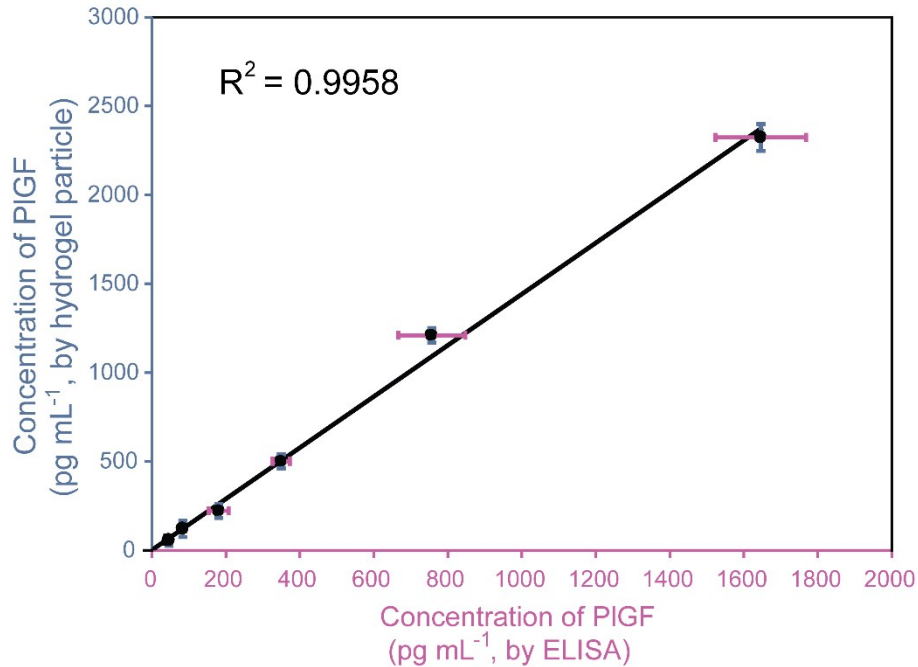


Figure S7. Comparison between hydrogel particle based colorimetric immunoassay and ELISA. Various concentrations of PIGF (62.5, 125, 250, 500, 1000, 2000 pg mL⁻¹) which satisfies the dynamic range of both methods, were spiked in healthy control plasma and measured by both methods. A linear correlation plot produced a slope of 1.44 and $R^2=0.9958$. As seen by correlation plot, ELISA underestimates the PIGF concentration with the recovery of 70-95%, while hydrogel particle based colorimetric immunoassay showed high accuracy with the recovery of 88.8-120.9%. Each data point and the vertical error bars represent the average signal and standard deviation of > 7 particles for hydrogel based colorimetric immunoassay and horizontal error bars represent the average signal and standard deviation of 3 wells for ELISA, respectively.

Table S1. The limit of detection and dynamic range of ELISA and hydrogel particle-based colorimetric immunoassays.

Target	Assay	Range [LOD-max.] (\log_{10})
PIGF	ELISA	[31.2 – 2,000 pg mL ⁻¹] (1.8)
	Hydrogel particle-based Colorimetric immunoassay	[41.3 – 7,500 pg mL ⁻¹] (2.3)
sFlt-1	ELISA	[125.0 – 8,000 pg mL ⁻¹] (1.8)
	Hydrogel particle-based Colorimetric immunoassay	[136.3 – 30,000 pg mL ⁻¹] (2.3)
sEng	ELISA	[125.0 – 8,000 pg mL ⁻¹] (1.8)
	Hydrogel particle-based Colorimetric immunoassay	[73.5 – 15,000 pg mL ⁻¹] (2.3)

Table S2. Multiplex detecton of PIGF, sFlt-1 and sEng and their recovery

Control Subtracted Signal (a.u.)

Case		PIGF		sFlt-1		sEng	Referenc
1	-	0 ± 0.69	-	0 ± 0.83	-	0 ± 0.47	[1] R. L. Dean, Biochem. <i>Mol. Biol.</i> <i>Educ.</i>
2	+	122.3 ± 2.52	-	-1.4 ± 1.14	-	-1.5 ± 0.9	
3	-	-0.5 ± 1.2	+	40.4 ± 1.01	-	0.1 ± 0.55	
4	+	111 ± 2.04	+	60.5 ± 1.3	-	-0.6 ± 0.6	
5	-	0.5 ± 0.97	-	1.5 ± 0.48	+	26.2 ± 2.16	
6	-	0.6 ± 0.89	+	48.8 ± 2.09	+	30.6 ± 2.6	
7	+	132.6 ± 2.63	-	0.5 ± 2.74	+	31.5 ± 1.2	
8	+	130.2 ± 2.91	+	69.4 ± 1.23	+	33.8 ± 3.96	
Avg.		124.03 ± 9.73		54.79 ± 12.77		30.50 ± 3.19	
Recov.(%)		122.93		125.2		92.56	

2002, **30**, 401.

- [2] N. W. Choi., et al. *Anal. Chem.* 2012, **84**, 9370.
- [3] K. M. Holtz, E. R. Kantrowitz. *FEBS Lett.* 1999, **462**, 7.
- [4] Appleyard, David C., Stephen C. Chapin, Patrick S. Doyle. *Anal. Chem.* 2011, **83**, 193.
- [5] Shapiro, Sarah J., Dhananjaya Dendukuri, Patrick S. Doyle. *Anal. Chem.* 2018, **90**, 13572.
- [6] Roh, Y. H., Lee, H. J., Moon, H. J., Kim, S. M., Bong, K. W. *Anal. Chim. Acta* 2019, **1076**, 110.
- [7] Sandrin, D., et al. *Phys. Chem. Chem. Phys.* 2016, **18**, 12860.
- [8] Landry, J. P., Ke, Y., Yu, G. L., and Zhu, X. D. *J. Immunol. Methods* 2015, **417**, 86.